Thomson-Backscattered X Rays From Laser-Accelerated Electrons

H. Schwoerer, B. Liesfeld,* H.-P. Schlenvoigt, K.-U. Amthor, and R. Sauerbrey

Institut für Optik und Quantenelektronik, Friedrich-Schiller-Universität, Max-Wien-Platz 1, 07743 Jena, Germany†

(Received 6 September 2005; published 10 January 2006)

We present the first observation of Thomson-backscattered light from laser-accelerated electrons. In a compact, all-optical setup, the ''photon collider,'' a high-intensity laser pulse is focused into a pulsed He gas jet and accelerates electrons to relativistic energies. A counterpropagating laser probe pulse is scattered from these high-energy electrons, and the backscattered x-ray photons are spectrally analyzed. This experiment demonstrates a novel source of directed ultrashort x-ray pulses and additionally allows for time-resolved spectroscopy of the laser acceleration of electrons.

DOI: 10.1103/PhysRevLett.96.014802 PACS numbers: 41.75.Jv, 52.27.Ny, 52.38.Hb, 52.38.Kd

The interaction of high-intensity lasers operating at near-infrared wavelengths with matter produces x-ray radiation with, in many aspects, unique properties. The primary processes of laser x-ray generation are the ionization of matter and the subsequent acceleration of electrons in the intense light field to high energies. Since the acceleration of the electrons is accomplished by an ultrashort and tightly focused laser pulse, all x-ray emissions have in common an ultrashort duration as well as a very small source size in the range of a few tens of μm^2.

The x-ray photon energies cover the entire spectrum from soft x rays to γ radiation: from deexcitation of highly ionized atoms in the multi-eV range [1], inner-shell radiation [2] in the keV range, to high-energy bremsstrahlung from relativistic electrons providing up to 100 MeV photons [3,4]. Recently, soft x rays originating from betatron oscillations of relativistic electrons in plasma channels were demonstrated [5]. The applications of laser-generated x rays comprise high-resolution lithography [6], time-resolved x-ray diffraction with atomic temporal and spatial resolution [7], and in recent times the triggering of nuclear reactions [8].

A different approach to generate ultrashort x-ray pulses with lasers is the scattering of an ultrashort laser pulse off a relativistic electron beam, which is called Thomson backscattering. The relativistic electron undergoes oscillations in the laser field, and the scattered light is detected in the laboratory. This scheme was experimentally demonstrated by crossing high-energy laser pulses with a picosecond relativistic electron beam from a conventional linear electron accelerator (LINAC) [9–11].

In this Letter we present the first purely laser-based femtosecond Thomson backscattering x-ray source, which was proposed a few years ago [12,13]. In contrast to the LINAC-based experiments the relativistic electrons are accelerated by an ultrashort, intense laser pulse, and the same laser delivers the photons to be scattered. The whole system is compact and jitter-free; it produces collimated x-ray pulses with keV photon energies and subpicosecond duration, which will be a novel, highly versatile source for ultrashort time-resolved x-ray spectroscopy.

The generated photon spectra, in turn, are closely related to the spectra of the electrons they were scattered from [12,14]. In fact, an all-optical setup as presented here permits one to monitor the temporal evolution of the electron spectra during the laser-acceleration process [15]. This is impossible using conventional diagnostic methods, e.g., magnet spectrometers that cover a small solid angle only and that must be placed outside the interaction region. The recent major advances in laser acceleration of electrons [16–18], which can to date be understood only through numerical simulations, manifest the need for such time-resolved and *in situ* diagnostics.

The experiment was performed with the Jena 10 terawatt Ti:sapphire laser JETI. It delivered laser pulses with a center wavelength of 800 nm, a pulse energy of 370 mJ on target, and a pulse duration of 85 fs. An intensity contrast ratio of 10^{-10} between amplified spontaneous emission and main laser pulse on a nanosecond time scale was achieved, deploying an additional fast pockels cell. The schematics of the experimental setup is shown in Fig. 1(a). The ultrashort laser pulse is divided by a 90/10 beam splitter into a pump pulse and a probe pulse, the stronger pump pulse being reflected from the beam splitter. Each of the pulses is focused by an F/2.5 45° off-axis parabolic mirror into a He gas jet. The pump pulse was focused to a nominal intensity of 2×10^{19} W/cm^2 and the weaker probe pulse to an intensity of 1×10^{18} W/cm^2. The laser field strength may also be expressed by the normalized vector potential $a_0 = eE/m_0\omega_L c$, where e is the electron charge, E the electric field amplitude, m_0 the electron rest mass, ω_L the laser frequency, and c the speed of light. a_0 amounts to 3 and 0.8 for the pump and probe pulse, respectively. The time delay between the laser pulses may be adjusted by moving the beam splitter as indicated in Fig. 1(a). The setup is located in a vacuum chamber and entirely computer controlled. The accurate adjustment of the spatial and temporal overlap of the two laser pulses was demonstrated and used for a single-shot autocorrelation measurement [19].

A cylindrical subsonic gas nozzle was used to create a pulsed He gas jet with a density profile of Gaussian shape

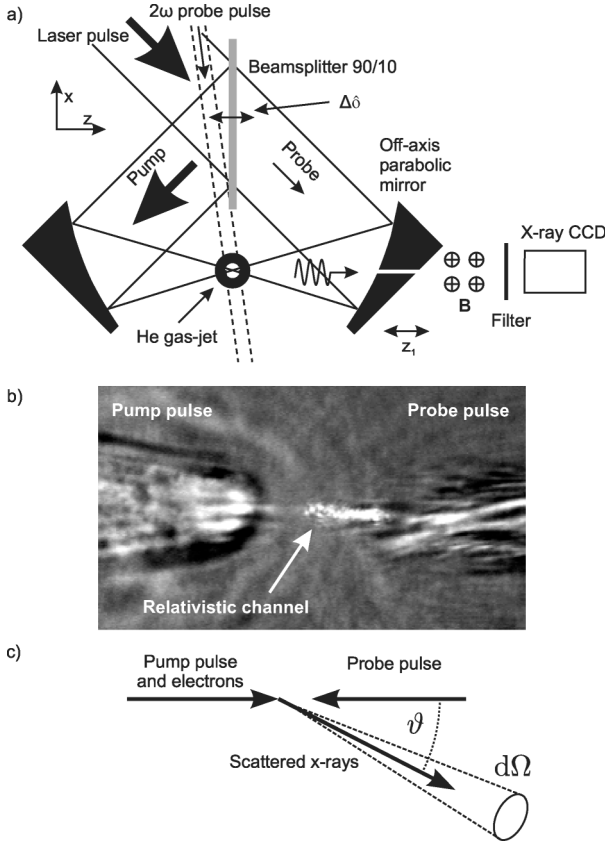

FIG. 1. (a) Setup of the Thomson-backscatter experiment: The main laser pulse is divided into two pulses by a 90/10 beam splitter both of which are focused by off-axis parabolic mirrors into a He gas jet. The backscattered radiation is observed with an x-ray CCD camera. A frequency-doubled laser pulse is used for shadowgraphy of the interaction region. (b) Shadowgram of the interaction region. The pump pulse is incident from the left generating the plasma channel, the probe pulse from the right. The bright area in the center of the image is due to the 2ω plasma self-emission within the relativistic channel, visible since the camera integrates over the entire interaction period. (c) Interaction scheme: ϑ is the angle of observation with respect to the electron propagation, and $d\Omega$ is the solid angle of detection.

along the laser axis and with a peak gas density of 6×10^{19} cm^{-3}. When focused into the rising edge of the He gas jet, the pump pulse undergoes relativistic self-focusing and generates a plasma channel. In this configuration electrons are efficiently accelerated in the forward direction to relativistic energies by direct laser acceleration [20] and self-modulated laser wakefield acceleration [21]. The spectrum of the high-energy electrons is dominated by an exponential shape and was determined in earlier experiments [22]. The temperature of the electron spectrum typically is of the order of 6 ± 1 MeV for our experimental parameters.

An ultrashort, frequency-doubled probe pulse with variable delay propagating at an angle of approximately 90° through the interaction region was deployed to record shadow images of the laser plasma with a time resolution of 100 fs. The same imaging setup was used to monitor the self-emission of the plasma at the second-harmonic frequency [22]. By monitoring the ionization fronts of the laser pulses in the shadow images, the spatial and temporal point of interaction of the laser pulses was reliably established. Figure 1(b) shows a typical shadowgram of the interaction region. The intensity of the pump pulse may considerably differ from the nominal intensity due to relativistic self-focusing. The probe beam, however, undergoes filamentation and is not capable of creating a single relativistic channel. The probe beam intensity may therefore be smaller than the nominal intensity of 10^{18} W/cm^2.

The probe pulse is scattered from accelerated high-energy electrons, and the backscattered x-ray photons are observed. A hole of 3 mm diameter was drilled into the parabolic mirror of the probe beam such that it is aligned with the axis of the focused beams. An x-ray CCD camera operating in single-photon counting mode was placed on this axis for energy-resolved detection of Thomson-backscattered photons. Each CCD image delivered a photon spectrum of a single laser shot in the range of 400 eV to 7 keV. The x-ray camera was shielded with a lead pinhole from background bremsstrahlung. A 300 nm nickel filter was introduced between x-ray CCD and laser focus to block irradiation by laser light. A pair of cylindrical dipole magnets was used to prevent electrons from reaching the x-ray CCD chip.

The scattered radiation field in terms of angular and energy density $d^2I/d\omega d\Omega$ may be explicitly calculated from the Lienard-Wiechert potentials [23]. Without significant loss of accuracy in the described experiment, we make the assumptions that the Lorentz factor of the electron is large ($\gamma^2 \gg 1$), that the solid angle of detection is small and close to the beam axis ($d\Omega \ll 1$, $\vartheta \ll 1$), and that the amplitude of the probe electromagnetic wave is small ($a_0^2 \ll 1$). In this case the scattered energy is equal to [12,14]

$$\frac{d^2I}{d\omega d\Omega} \approx r_e m_0 c \gamma^2 N_0^2 a_0^2 \left(\frac{\omega}{4\gamma^2 \omega_L}\right)^2 R(\omega, \omega_L), \qquad (1)$$

where the angular distribution function R is given by

$$R(\omega, \omega_L) = \mathrm{sinc}^2\left(\frac{\bar{k}L}{2}\right), \qquad \bar{k} = \frac{\omega}{c}\left(\frac{1 + \gamma^2\vartheta^2}{4\gamma^2}\right) - \frac{\omega_L}{c}. \qquad (2)$$

Here, ω is the frequency of the scattered photon, ω_L the laser frequency, N_0 the number of laser oscillations of the probe pulse, and $L = N_0\lambda_L$ the interaction length. $r_e = e^2/(4\pi\varepsilon_0 m_0 c^2)$ is the classical electron radius and ϑ the angle of observation with respect to the optical axis [see Fig. 1(c)].

The maximum photon energy of $E_{\max} = 4\gamma^2\hbar\omega_L$ is emitted in forward direction. The opening angle of the emission is determined by $\vartheta_c \approx (1/(\gamma\sqrt{N_0})$. The faster the electron and the longer the modulation of the electron in the electromagnetic wave, the smaller the emission cone

of the Thomson scattered x rays. As an example, in case of a 5 MeV electron ($\gamma \approx 10$) and 30 laser oscillations, corresponding to an 80 fs probe pulse, the expected x-ray photon energy in forward direction is 620 eV and the opening half angle of the central emission cone is $\vartheta_c \approx 0.02$ rad.

In order to adequately interpret the observed x-ray spectra, we note that under the conditions of uncontrolled trapping in the relativistic channel the accelerated electrons have a broad energy distribution $N_b\Phi(\gamma) = m_0c^2 dN_e/dE_e$, where N_b is the total number of electrons in the accelerated bunch. We therefore integrate the scattered energy density in Eq. (1) over $\Phi(\gamma)$, respecting the energy dependent emission cone. Experimentally, the photon collection solid angle was $\Delta\Omega \approx 80\ \mu$sr and we may assume that the photon distribution is flat over this angle. It may be shown that the measured x-ray photon density is then equal to [12]

$$\frac{dN_x(E_x)}{dE_x} = \frac{\alpha_f}{8E_L} a_0^2 N_b N_0 \gamma \Phi(\gamma) \Delta\Omega, \tag{3}$$

where $E_x = \hbar\omega$ is the x-ray photon energy, $E_L = \hbar\omega_L$ the laser photon energy, and α_f the fine structure constant. As a result, the energy of the emitted x-ray photons varies in a rather wide range, forming a continuum extending from zero to an energy of a few keV. Since γ is a function of ϑ, the observed photon spectrum is strongly dependent on the angle of observation ϑ.

A typical Thomson-backscattered x-ray spectrum is shown in Fig. 2(a). In the particular case shown, ϑ was experimentally determined to 60 mrad and the delay of the probe with respect to the pump pulse was set to be 200 fs. The total number of Thomson-backscattered x-ray photons was about 30 000 per shot in the range of 430 to 2030 eV. Since the observation angle ϑ was nonzero it follows from Eqs. (2) and (3) that a much larger number of photons is expected in forward direction ($\vartheta = 0$) [12]. Figure 2(b) shows the electron spectrum derived from Fig. 2(a) according to Eq. (3). The electron spectrum exhibits two Boltzmann components of temperatures of 1.3 and 6.1 MeV. The electron temperatures do not change significantly varying the pump-probe delay, which is equivalent to scanning the acceleration process in the plasma channel.

The experimental evidence that the measured x-ray spectrum as shown in Fig. 2(a) is Thomson-backscattered radiation is based on three measurements: (1) From

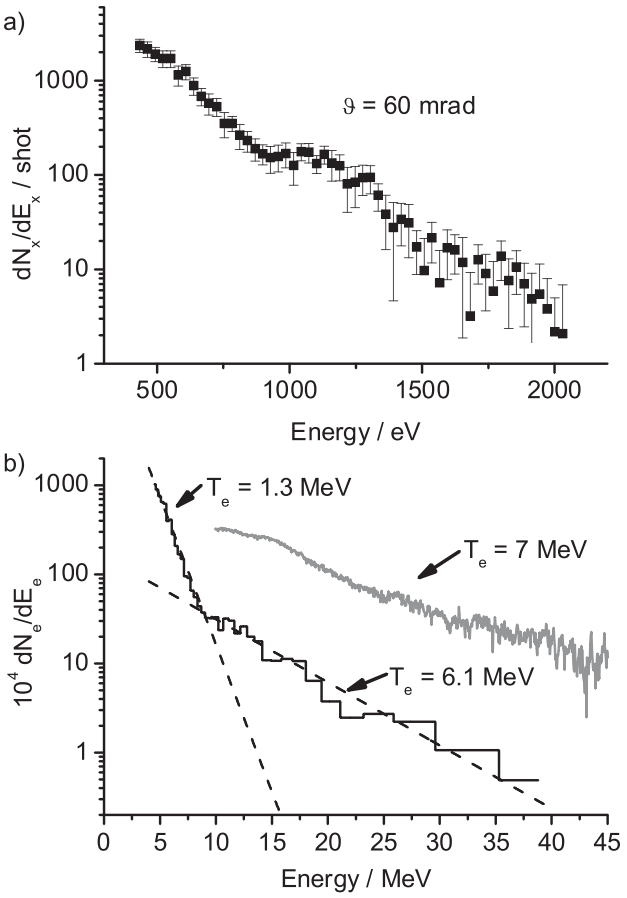

FIG. 2. (a) Typical Thomson-backscattered photon spectrum recorded with the x-ray CCD camera at a delay between pump and probe pulse of 200 fs averaged over 10 laser shots. The error bars indicate the standard error for a single channel derived from the fluctuations of 10 shots. The spectrum is corrected for background and filter transmission. (b) Solid line: electron spectrum obtained from photon spectrum in (a) according to Eq. (3). For comparison, an electron spectrum recorded with a conventional magnet spectrometer under similar conditions is shown as a gray line (rescaled for visibility) [24].

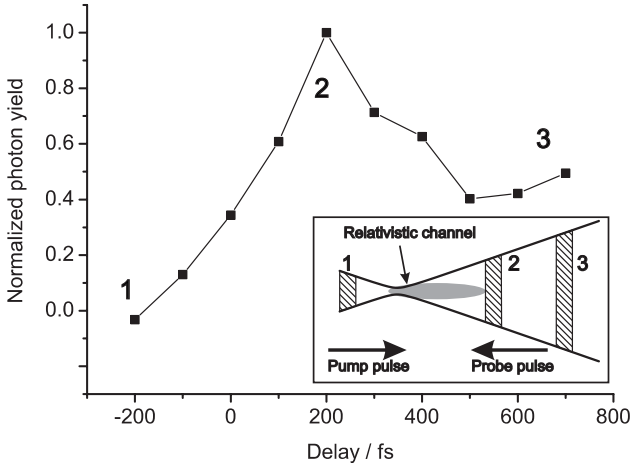

FIG. 3. Varying the delay between pump and probe pulse: The integral number of photons in the interval 430 to 2030 eV averaged over 10 laser shots is plotted over the delay between the laser pulses. The number of photons was normalized to the peak of the respective curves to facilitate comparison between data recorded under varying circumstances. A delay of 0 fs corresponds to both pulses interacting in their common focus. Inset: Sketches of three scenarios of different pump-probe delay where the pump pulse is incident from the left generating a relativistic channel. The region where pump and probe pulse overlap is indicated by a hatched box.

Ref. [5] it is known that the pump pulse itself might produce radiation in a similar energy range originating from betatron oscillations of the relativistic electrons inside the plasma channel. In order to distinguish between the two competing mechanisms, the spectrum generated by the pump pulse only and consisting of betatron radiation and bremsstrahlung of electrons hitting the aluminum parabola and the steel vacuum vessel walls was recorded. The Thomson spectrum, as displayed in Fig. 2, was identified as the difference between the spectra recorded with and without the probe pulse. The Thomson signal is orders of magnitude larger than shot-to-shot fluctuations in the low energy range and the signal-to-background ratio amounts to 30%.

(2) Another independent indication of the origin of the signal is its dependence on the delay between the electron-accelerating pump pulse and the probe pulse. The integral number of photons in the energy interval from 430 to 230 eV for varying delay between the pulses is displayed in Fig. 3. At a negative time delay corresponding to the situation that the probe pulse passed the focus before the pump pulse arrived (i.e., before the formation of a relativistic channel), the integral signal is zero. Towards positive delay the number of backscattered photons increases to a maximum at 200 fs and then slowly decreases again. This dependency was verified in several experiments under varying conditions. To our knowledge, there is no other source of x-ray radiation besides Thomson backscattering that could possibly exhibit such a dependency on the time delay on such a short time scale. We attribute the strong increase in photon number between -200 and 200 fs to the ongoing process of electron acceleration in the relativistic channel. Electron acceleration starts at a negative delay in our frame of reference since the pump pulse undergoes self-focusing. After 400 fs this process is complete and the decrease of signal is due to the divergence of both the electron beam and the probe pulse. (3) Finally, the high temperature component in the electron spectrum obtained from Thomson backscattering is in agreement with earlier measurements using a conventional magnet spectrometer [see Fig. 2(b)].

We demonstrated the first experimental observation of Thomson-backscattered radiation in a versatile all-optical setup, the photon collider. The Thomson radiation, generated by scattering laser photons from counterpropagating laser-accelerated electrons, was spectrally characterized in the range of 0.4 to 2 keV. The x-ray spectra provide unique direct and time-resolved information about the electron distribution function and the acceleration process inside an underdense laser plasma. Future experiments will be extended towards backscattering from quasimonoenergetic electron bunches yielding narrow-band, ultrashort, and extremely bright x-ray beams in the several hundred keV range.

We thank B. Beleites, K. Haupt, A. Debus, F. Ronneberger, and W. Ziegler for assistance and A. Nazarkin for useful discussions. This work was supported by DFG priority Project No. TR-18.

*Electronic address: liesfeld@ioq.uni-jena.de
†Electronic address: http://www.physik.uni-jena.de/qe

[1] S. Sebban *et al.*, IEEE J. Sel. Top. Quantum Electron. **10**, 1351 (2004).
[2] F. Ewald, H. Schwoerer, and R. Sauerbrey, Europhys. Lett. **60**, 710 (2002).
[3] H. Schwoerer, P. Gibbon, S. Düsterer, R. Behrens, C. Ziener, C. Reich, and R. Sauerbrey, Phys. Rev. Lett. **86**, 2317 (2001).
[4] Y. Glinec *et al.*, Phys. Rev. Lett. **94**, 025003 (2005).
[5] A. Rousse *et al.*, Phys. Rev. Lett. **93**, 135005 (2004).
[6] U. Stamm, J. Phys. D **37**, 3244 (2004).
[7] K. Sokolowski-Tinten and D. von der Linde, J. Phys. Condens. Matter **16**, R1517 (2004).
[8] K. W. D. Ledingham, P. McKenna, and R. P. Singhal, Science **300**, 1107 (2003).
[9] R. Schoenlein, W. Leemans, A. Chin, P. Volfbeyn, T. Glover, P. Balling, M. Zolotorev, K. Kim, S. Chattopadhyay, and C. Shank, Science **274**, 236 (1996).
[10] M. Yorozu, J. Yang, Y. Okada, T. Yanagida, F. Sakai, K. Takasago, S. Ito, and A. Endo, Appl. Phys. B **74**, 327 (2002).
[11] D. J. Gibson *et al.*, Phys. Plasmas **11**, 2857 (2004).
[12] P. Catravas, E. Esarey, and W. Leemans, Meas. Sci. Technol. **12**, 1828 (2001).
[13] N. Hafz, H. Lee, J. Kim, G. Kim, H. Suk, and J. Lee, IEEE Trans. Plasma Sci. **31**, 1388 (2003).
[14] E. Esarey, S. K. Ride, and P. Sprangle, Phys. Rev. E **48**, 3003 (1993).
[15] P. Tomassini, M. Galimberti, A. Giulietti, D. Giulietti, L. A. Gizzi, and L. Labate, Phys. Plasmas **10**, 917 (2003).
[16] S. P. D. Mangles *et al.*, Nature (London) **431**, 535 (2004).
[17] C. G. R. Geddes, C. Toth, J. v. Tilborg, E. Esarey, C. B. Schroeder, D. Bruhwilder, C. Nieter, J. Cary, and W. P. Leemans, Nature (London) **431**, 538 (2004).
[18] J. Faure, Y. Glinec, A. Pukhov, S. Kiselev, S. Gordienko, E. Lefebvre, J. P. Rousseau, F. Burgy, and V. Malka, Nature (London) **431**, 541 (2004).
[19] B. Liesfeld, J. Bernhardt, K.-U. Amthor, H. Schwoerer, and R. Sauerbrey, Appl. Phys. Lett. **86**, 161107 (2005).
[20] C. Gahn, G. D. Tsakiris, A. Pukhov, J. Meyer-ter Vehn, G. Pretzler, P. Thirolf, D. Habs, and K. J. Witte, Phys. Rev. Lett. **83**, 4772 (1999).
[21] A. Modena *et al.*, Nature (London) **377**, 606 (1995).
[22] B. Liesfeld, K.-U. Amthor, F. Ewald, H. Schwoerer, J. Magill, J. Galy, G. Lander, and R. Sauerbrey, Appl. Phys. B **79**, 1047 (2004).
[23] J. D. Jackson, *Classical Electrodynamics* (Wiley, New York, 1999), 3rd ed.
[24] B. Hidding *et al.* (to be published).